A MICROSCOPIC STUDY ON SHEAR MECHANISM OF GRANULAR MATERIALS IN SIMPLE SHEAR SIMULATED BY DEM

Hajime Matsuoka[i], Sihong Liu[ii], Yusuke Ueno[iii] and Hitoshi Kodama[iii]

ABSTRACT

By using a special two-dimensional simple shear test apparatus with rigid side plates, simple shear tests on assemblies of aluminum rods (3mm and 5mm in diameters, 50mm in length and mixing ratio 3:2 by weight) are carried out. Then, these tests are simulated by DEM. The simulation results by DEM agree well with the test results. Based on the simulation results, the stress-dilatancy relation of granular materials is studied from a microscopic view by taking the distribution of the interparticle contact forces into account. And the shear mechanism of granular materials in simple shear test, such as the frequency distribution of the change in contact orientations of particles along the mobilized plane and the factors affecting it, is also studied.

Key words: dilatancy, distinct element method, fabric, granular material, microscopy, simple shear (**IGC:** D6/E13)

INTRODUCTION

Macroscopic mechanical features of granular materials are closely related to the behavior of individual particles. So far, many studies have been performed on the micromechanics and the macroscopic response of granular materials under shear. For example, Oda and Konishi(1974) carried out simple shear tests on assemblies of photoelastic rods and found that the frequency distribution of contact orientations of granular materials tends to concentrate around the major principal stress axis. Matsuoka(1974) performed direct box shear tests on assemblies of aluminum and photoelastic rods and derived the relationship between shear-normal stress ratio and normal-shear strain increment ratio on the mobilized plane by taking the change in the frequency distribution of contact orientations into account. Recently, distinct element method (DEM) has been widely used to study micromechanics of granular materials because it has a great merit that the displacements, the contact forces, the contact orientations of particles and so on can be calculated easily and exactly. Yamamoto et al.(1994,1995) simulated numerically biaxial compression tests on assemblies of aluminum rods by DEM and found from the micromechanical observation that the distribution of the change in interparticle contact angles is proportional to the distribution of macroscopic shear-normal stress ratio on the contact plane. In this paper, another type of tests, simple shear test, is simulated numerically by DEM, and based on the simulation results, the shear mechanism of granular materials in simple shear test is studied from a microscopic view.

Firstly, using a special two-dimensional simple shear test apparatus with two rigid side plates, simple shear tests with two kinds of specimen heights (4.9cm and 9.8cm) are carried out on assemblies of aluminum rods. Then, these tests are simulated by DEM. Based on the simulation results, the stress-dilatancy relation of granular materials, which is one of the most important relations in building constitutive laws for soil, is studied from a microscopic view by taking the frequency distribution of the interparticle contact forces into account. And the change law of contact orientations on the mobilized plane found by Yamamoto et al.(1994,1995) in the biaxial compression test is also confirmed in simple shear test. Furthermore, the change in contact orientations during shear and its mechanism are also studied.

SIMULATION OF SIMPLE SHEAR TESTS BY DEM

Figure 1 shows a special two-dimensional simple shear test apparatus. In this apparatus, the lateral

i) Professor, Department of Civil Engineering, Nagoya Institute of Technology,Nagoya,466-8555.
ii) Graduate Student of Doctor Course, ditto.
iii) Graduate Student, ditto.

walls are two rigid plates that are connected to the base plate with two hinges and also connected by a rigid bar at the upper backside with two hinges. Therefore, the same shear strains (rotation angle of the lateral walls) can always be kept on the left wall and on the right wall. The upper loading plate on the specimen is pulled horizontally under the application of a constant vertical load, resulting in the inclination of the lateral walls and production of the shear strain. The simple shear tests are carried out on assemblies of aluminum rods with 3mm and 5mm in diameters, 50mm in length and 3:2 in mixing ratio by weight. A layer of the same aluminum rods as the specimen is pasted on the base of the upper loading plate and the bottom of the shear box in order to make them have sufficient frictional resistance. Two kinds of the specimen dimensions are selected: one is 20cm in width and 4.9cm in height (case 1); the other is 20cm in width and 9.8cm in height (case 2). The normal stress and the initial void ratio of the specimen are respectively equal to 52kPa and 0.201 either in case 1 or in case 2.

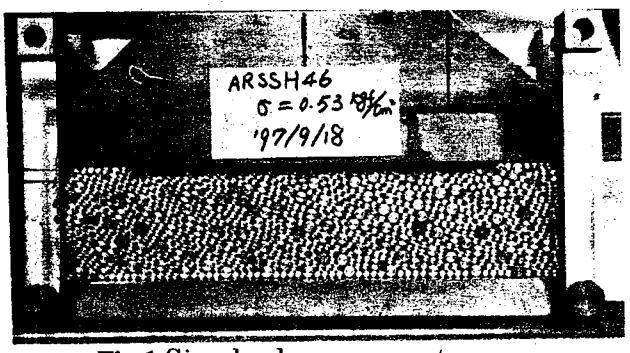

Fig.1 Simple shear apparatus

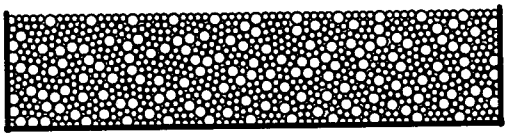

Fig.2 Arrangement of initial particles used in DEM simulation (case 1)

Table 1. Input parameters for numerical simulation by DEM

	Particle-particle	*Particle-plate*
Normal stiffness k_N, k_N'(N/m/m)	9.0×10^9	1.8×10^{10}
Shear stiffness k_S, k_S'(N/m/m)	3.0×10^8	6.0×10^8
Normal damping η_N,η_N'(N s/m/m)	7.9×10^4	1.1×10^5
Shear damping η_S,η_S'(N s/m/m)	1.4×10^4	2.0×10^4
Friction angle ϕ_μ, ϕ_μ' (deg.)	16	16
Density of particles ρ (kg/m^3)	2700	
Time increment Δt (sec.)	2×10^{-7}	

Figure 2 shows the initial particle arrangement used in DEM simulation corresponding to the case 1, which was digitized from the picture as shown in **Fig.1**. **Table 1** gives the input parameters for DEM simulation. **Figure 3** illustrates the relationships among the shear -normal stress ratio (τ/σ_N), the shear strain (γ) and the normal strain (ε_N), in which the plots represent the experimental results and the lines represent the results obtained by DEM simulation. As seen from **Fig. 3,** the numerical results agree well with the experimental results either in case 1 or in case 2. Since two lateral rigid plates on the left and on the right are inclined at the same angle (shear strain) caused by pulling the upper loading plate horizontally as mentioned above, therefore, it is natural to assume that the orientation of the sliding plane is horizontal. **Figure 4** shows the distribution of the displacement vectors

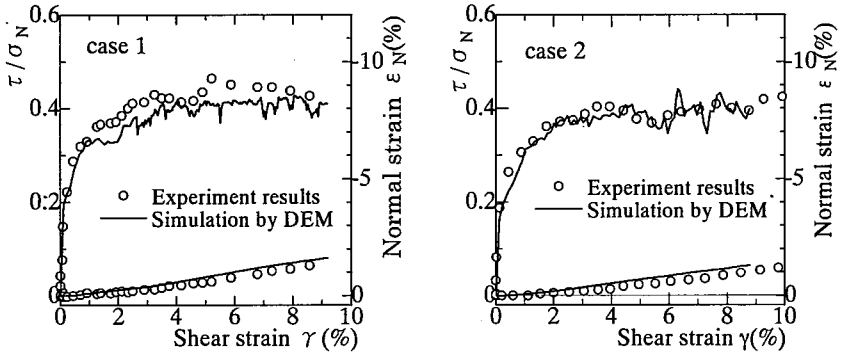

Fig.3 Comparison between experiment results and simulation results by DEM

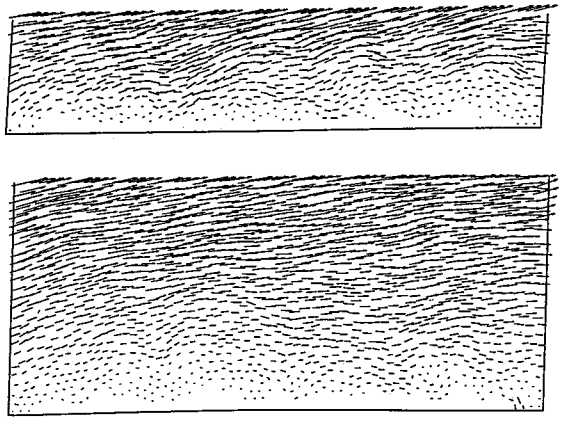

Fig.4 Displacement vectors up to about the peak strength

from the beginning of shearing to the peak strength. **Figure 5** shows the distribution of the average horizontal displacement at every 5cm of the specimen width along the specimen height, in which the solid lines correspond to the deformation of the rigid plate (either the left or the right), and the plots represent the results of the numerical simulation. It can be seen from **Figs. 4 and 5** that the horizontal displacements within the specimen are almost the same as those of the lateral plates at the same level, in other words, the shear strains through the specimen are reasonably uniform. Furthermore, we can calculate the average stresses in the whole specimen from the interparticle contact forces using the formula:

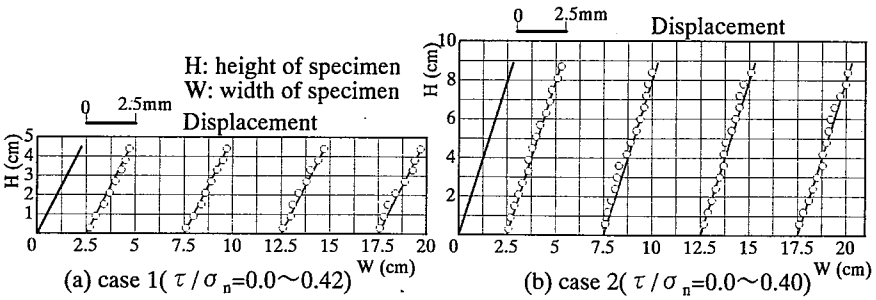

Fig.5 Horizontal displacement along specimen height at every 5cm span of specimen width

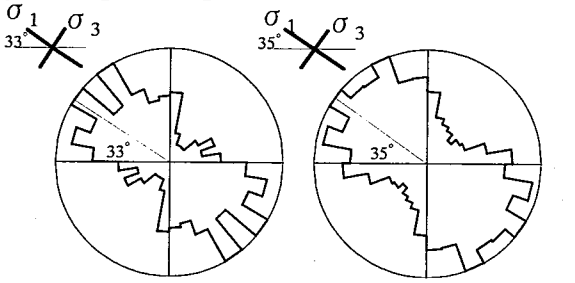

Fig.6 Orientations of principal stresses at peak strength calculated from contact forces

$$\sigma_{ij} = \left(\sum_{R} \ell_i F_j\right) / V$$

(Christoffersen et al.,1981), where R is the calculation domain, V is the volume of the domain, ℓ_i is the length of vectors connecting the centers of contacting particles, and F_j is the contact force. It was found that, at peak strength, the major principal stress calculated by the above formula are inclined to the horizontal plane at an angle of about 33° in case 1 and about 35° in case 2 (see **Fig. 6**). On the other hand, as the internal friction angle ϕ of aluminum rod mass is about 22° ~24° , the angle between the major principal stress and the mobilized plane is equal to $\pi/4-\phi/2$=33° ~34° , which agrees nearly the angle obtained from the contact forces. By taking the above two facts into account, therefore, we can assume that the mobilized plane is nearly horizontal. Next, the shear mechanism of granular materials in simple shear test will be studied on this assumption.

SHEAR MECHANISM OF GRANULAR MATERIALS IN SIMPLE SHEAR

Stress-dilatancy Relation on mobilized plane

The stress-dilatancy relation is one of the most important relations in the constitutive equation for granular materials. Through the direct box shear tests on aluminum and photoelastic rod mass, Matsuoka (1974) derived a stress-dilatancy relation on the mobilized plane by taking the distribution of interparticle contact angles into account. Yamamoto et al. (1994,1995) examined this relation from a microscopic view on the basis of the simulation results by DEM for biaxial compression tests on aluminum rod mass. Herein, based on the above-stated simulation results by DEM for simple shear tests on aluminum rod mass, we examine this relation again by taking not only the distribution of interparticle contact angles but also the distribution of interparticle contact forces into account.

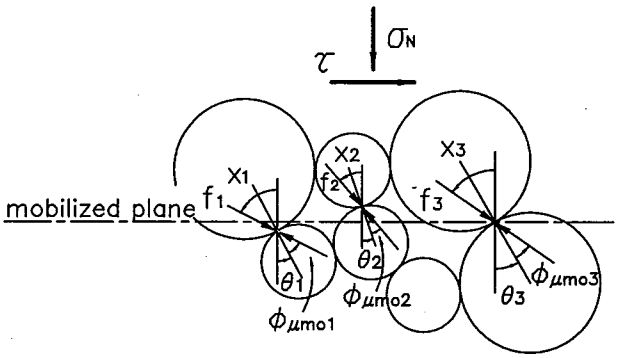

Fig.7 Equilibrium of inter-particle contact forces on the mobilized plane

Paying attention to the interparticle contacts along the mobilized plane as shown in **Fig. 7** and denoting the interparticle contact angle by θ_i, the interparticle contact force by f_i and the

mobilized interparticle friction angle by $\phi_{\mu moi}$, we can obtain the following equation from the equilibrium of interparticle forces on the mobilized plane.

$$\frac{\tau}{\sigma_N}=\frac{\sum_{i=1}^{n} f_i(\theta_i+\phi_{\mu moi})\sin(\theta_i+\phi_{\mu moi})}{\sum_{i=1}^{n} f_i(\theta_i+\phi_{\mu moi})\cos(\theta_i+\phi_{\mu moi})}=\frac{\sum_{i=1}^{n} f_i(x_i)\sin x_i}{\sum_{i=1}^{n} f_i(x_i)\cos x_i} \qquad (1)$$

where n means the number of the interparticle contacts along the mobilized plane and $x_i(=\theta_i+\phi_{\mu moi})$ means the angle between the interparticle contact force f_i and the normal to the mobilized plane. The angle x_i changes from $-\pi/2$ to $\pi/2$. Replacing $f_i(x_i)$ approximately with a frequency distribution function of interparticle contact forces F(x), Eq.(1) can be rewritten as follows:

$$\frac{\tau}{\sigma_N}=\frac{\int_{-\pi/2}^{\pi/2} F(x)\sin x\,dx}{\int_{-\pi/2}^{\pi/2} F(x)\cos x\,dx}\cong\tan\bar{x} \qquad (2)$$

where $\bar{x}=\dfrac{\int_{-\pi/2}^{\pi/2} F(x)\,x\,dx}{\int_{-\pi/2}^{\pi/2} F(x)\,dx}$

On the other hand, the relation between the normal-shear strain increment ratio ($-d\varepsilon_N/d\gamma$) and the average interparticle contact angle $\bar{\theta}$ is expressed as follows(Matsuoka,1974; Yamamoto et al.,1994):

$$-\frac{d\varepsilon_N}{d\gamma}=\frac{\int_{-\pi/2}^{\pi/2} N(\theta)\sin\theta\,d\theta}{\int_{-\pi/2}^{\pi/2} N(\theta)\cos\theta\,d\theta}\cong\tan\bar{\theta} \qquad (3)$$

where $\bar{\theta}=\dfrac{\int_{-\pi/2}^{\pi/2} N(\theta)\,\theta\,d\theta}{\int_{-\pi/2}^{\pi/2} N(\theta)\,d\theta}$ and $N(\theta)$ denotes the frequency distribution of interparticle contact angles.

Figure 8 shows the relationships among $\bar{x}$, $\bar{\theta}$ and shear strain γ obtained from the numerical results of the simple shear tests on aluminum rod mass by DEM. It is seen from **Fig.8** that the $\bar{x}$ vs. γ relationship is similar to the $\bar{\theta}$ vs. γ relationship and the difference between $\bar{x}$ and $\bar{\theta}$ varies very slightly with the increase in the shear strain, independent of the specimen height (case 1 and case 2). In the case of our simulation results of simple shear tests on aluminum rod mass, this difference is about 7° . If we denote this difference by δ, we can obtain

$$\bar{x}=\bar{\theta}+\delta \qquad (4)$$

Next, we consider the reason of the difference δ . **Figure 9** shows the normalized frequency distribution $N(\theta)$ of interparticle contact angles and the normalized frequency distribution F(x) of

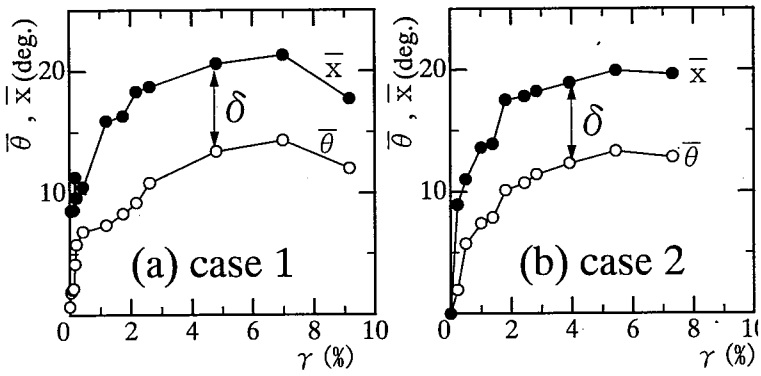

Fig.8 Relationships among $\bar{x}$, $\bar{\theta}$ and γ on mobilized plane

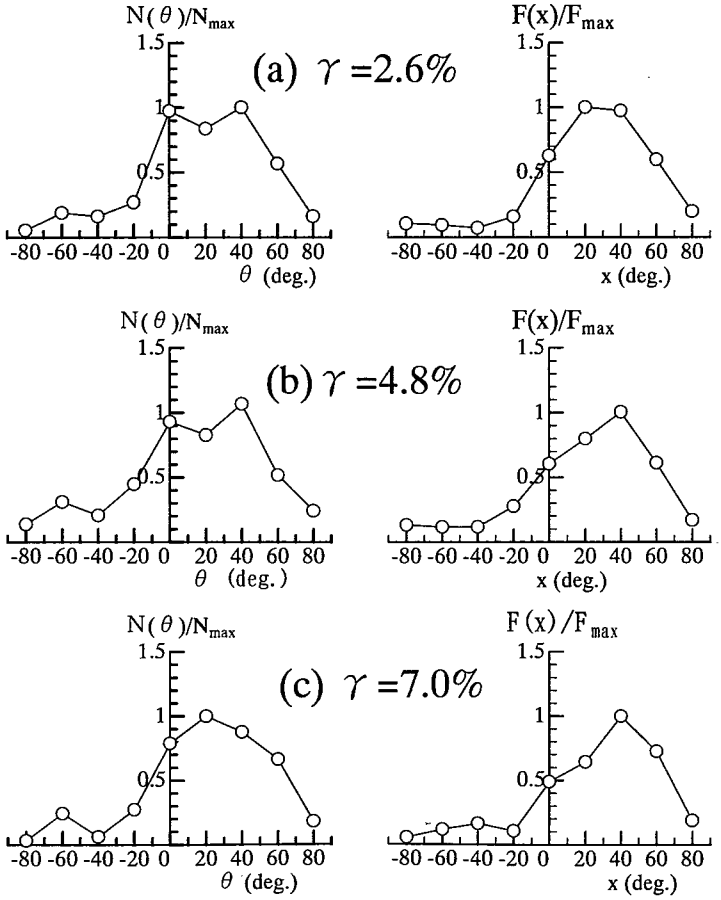

Fig.9 Frequency distribution of interparticle contact angles $N(\theta)$ and interparticle contact forces F(x) on mobilized plane at different shear strains in case 1 as shown in Fig.8(a)

interparticle contact forces at three different shear strains in case 1 as shown in **Fig.8(a)**. As seen from **Fig.9**, both the distribution curve of N(θ) and the distribution curve of F(x) are unsymmetrical being inclined toward the right side—the positive zone of θ and x. However, the distribution curve of F(x) is well inclined toward the right side than the distribution curve of N(θ), and this tendency is the same at different shear strains. This is considered to be the reason of the difference δ.

From Eqs.(2), (3) and (4), the relationship between the shear-normal stress ratio(τ / σ_N) and normal-shear strain increment ratio ($-d\varepsilon_N/d\gamma$) can be obtained:

$$\frac{\tau}{\sigma_N} \cong \tan\bar{x} = \tan(\bar{\theta}+\delta) = \frac{\tan\bar{\theta}+\tan\delta}{1-\tan\bar{\theta}\cdot\tan\delta} = \frac{1+\tan^2\delta}{1-\tan\bar{\theta}\cdot\tan\delta}\tan\bar{\theta}+\tan\delta$$
$$= \frac{1+\tan^2\delta}{1+\tan\delta\cdot\left(\frac{d\varepsilon_N}{d\gamma}\right)}\left(-\frac{d\varepsilon_N}{d\gamma}\right)+\tan\delta$$
$$\cong \lambda\left(-\frac{d\varepsilon_N}{d\gamma}\right)+\mu \qquad (5)$$

where λ and μ (= $\tan\delta$) are soil parameters. As $\bar{x}$ ($=\overline{\theta_i+\phi_{\mu moi}}$) is the average value of the angles between the interparticle contact force and the normal to the mobilized plane (Eq.2) and $\bar{\theta}$ is the average value of interparticle contact angles (Eq.3), it is seen from Eq.4 that μ (= $\tan\delta$) is caused by the distribution difference between interparticle contact forces F(x) and interparticle contact angles N(θ) as shown in **Fig.9**. If the distribution of interparticle contact forces F(x) is similar to that of interparticle contact angles N(θ), and the mobilized interparticle friction angle $\phi_{\mu moi}$ for each contact is assumed to be equal to the average value of all contacts ($\bar{\phi}_{\mu mo}$), $\bar{x}$ ($=\overline{\theta_i+\phi_{\mu moi}}$) becomes ($\bar{\theta}+\bar{\phi}_{\mu mo}$) and μ (=$\tan\delta$ =$\tan(\bar{x}-\bar{\theta})$) becomes $\tan\bar{\phi}_{\mu mo}$. In the previous study (Yamamoto et al.,1994), the parameter μ in Eq.(5) was equal to $\tan\bar{\phi}_{\mu mo}$.

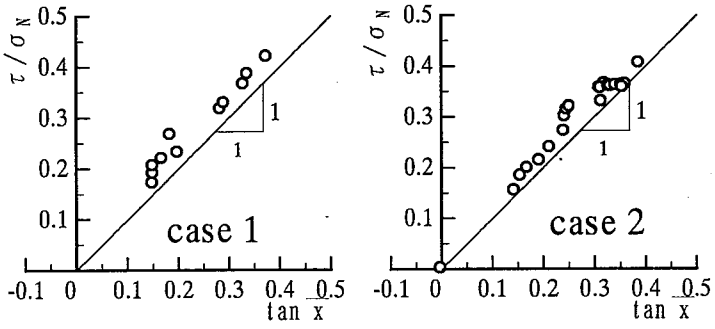

Fig.10 Macroscopic τ / σ_N vs. microsocopic $\tan\bar{x}$ relationship on mobilized plane

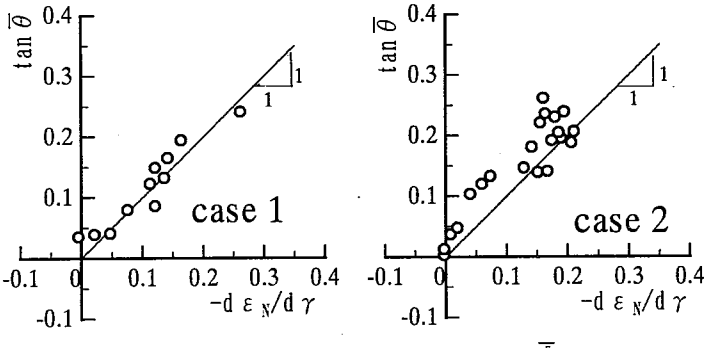

Fig.11 Macroscopic $-d\varepsilon_N/d\gamma$ vs. microsocopic $\tan\bar{\theta}$ relationship on mobilized plane

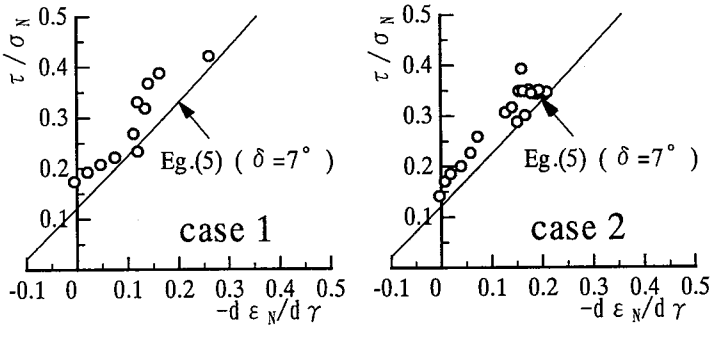

Fig.12 Macroscopic τ / σ_N vs. macroscopic $-d\varepsilon_N/d\gamma$ relationship on mobilized plane

Figures 10, 11 and 12 present the relationships corresponding to Eqs.(2), (3) and (5), respectively, in which plots ○ represent the simulation results of the simple shear test by DEM. It is seen from **Fig.10** that the plot corresponding to the macroscopic quantity of τ / σ_N and the microscopic quantity of $\tan\bar{x}$ is in approximate agreement with the expression of Eq.(2) either in case 1 or in case 2. It is also seen from **Fig.11** that the plot corresponding to the macroscopic quantity of $-d\varepsilon_N/d\gamma$ and the microscopic quantity of $\tan\bar{\theta}$ is in approximate agreement with the expression of Eq.(3) either in case 1 or in case 2. In **Fig.12**, the solid line represents the expression of Eq.(5) when $\delta = 7°$. It is seen from **Fig.12** that the plots corresponding to the macroscopic quantities of τ / σ_N and $-d\varepsilon_N/d\gamma$ are approximately arranged on the line expressed by Eq.(5) either in case 1 or in case 2, which provides an indication that the stress-dilatancy relation of granular materials can be

expressed by Eq.(5).

The above experimental and numerical tests (cases 1 and 2) are all carried out at the initial void ratio e_0 of 0.201. To verify the above equations at a looser state, we simulate another case with a specimen height of 9.8cm and an initial void ratio e_0 of 0.233 by DEM. **Figure 13** shows: (a) the relationships among $\bar{x}$, $\bar{\theta}$ and shear strain γ; and (b) the relationship between the macroscopic quantity of τ / σ_N and the microscopic quantity of $\tan\bar{x}$ at the loose state (e_0=0.233). The following two things can be seen from **Fig.13**: (1)the difference δ ($=\bar{x}-\bar{\theta}$) is also almost changeless during shear at the loose state(e_0=0.233),and the value is also about 7° on the average, the same as that at the initial void ratio e_0 of 0.201(case 1 and case 2); (2) the plots corresponding to the macroscopic quantity of τ / σ_N and the microscopic quantity of $\tan\bar{x}$ are also approximately arranged on the line expressed by Eq.(2) at the loose state. At the loose state, as there is a great fluctuation in the stress-strain response, it is difficult to calculate the normal-shear strain increment ratio $-d\varepsilon_N/d\gamma$ so that the relationships expressed by Eqs.(3) and (5) are not given.

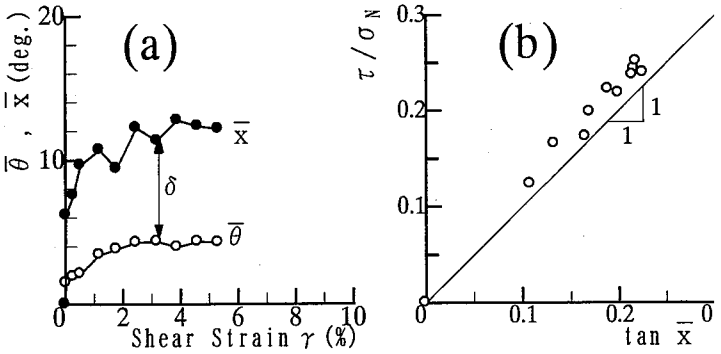

Fig.13 Results on the mobilized plane at loose state(e_0=0.233): (a) relationships among $\bar{\theta}$, $\bar{x}$ and γ; (b)relationship between τ / σ_N and $\tan\bar{x}$

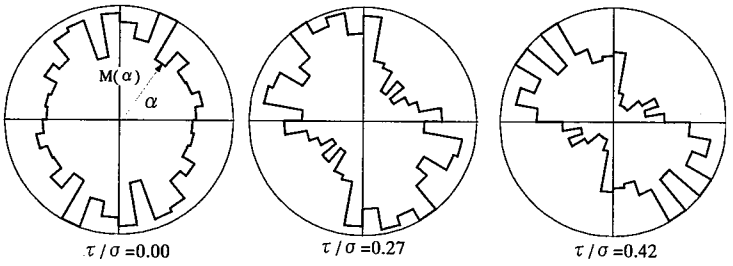

Fig.14 Frequency distribution of contact normal orientations during shear(case 1)

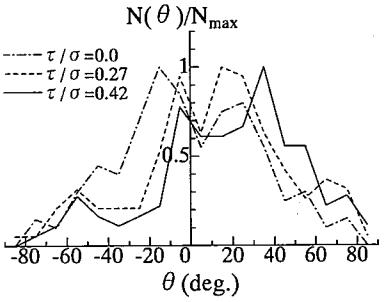

Fig.15 Variation of interparticle contact angles on mobilized plane during shear (case 1)

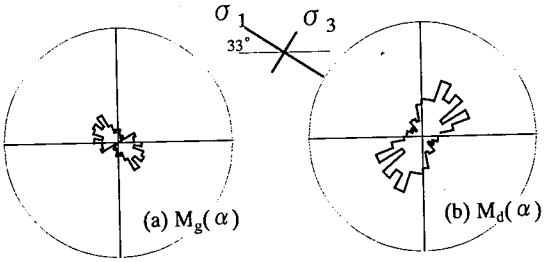

Fig.16 Frequency distribution of contact normal orientations(case 1): (a) "generated contacts" $M_g(\alpha)$, (b) "disappearing contacts" $M_d(\alpha)$

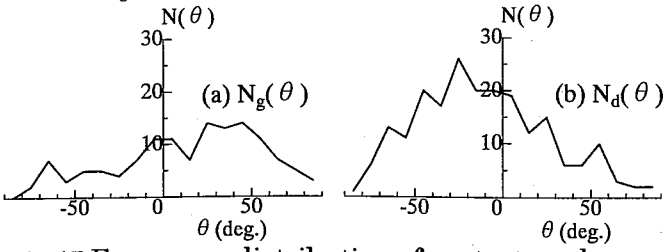

Fig.17 Frequency distribution of contact angles on mobilized plane(case 1): (a)for "generated contacts", $N_g(\theta)$; (b) for "disappearing contacts", $N_d(\theta)$.

Change in Contact Normal Orientations

Figure 14 shows the frequency distribution of contact normals $M(\alpha)$ during shear in case 1, where α denotes the inclination angle of the contact normal to the horizontal plane. As shown in **Fig.14**, the contact normals $M(\alpha)$ tend to concentrate toward a preferred direction which gradually rotates with the increase in shear stress. This preferred direction of contact normals agrees nearly with the major principal stress direction, as reported by Oda et al.(1974). **Figure 15** shows the normalized frequency distribution of interparticle contact angles $N(\theta)/N_{max}$ on the mobilized plane using the same data as **Fig.14**, where θ is the interparticle contact angle, namely, the angle between the contact plane and the mobilized plane. It is seen from **Fig.15** that, with the increase in shear-normal stress ratio τ / σ_N, the distribution of $N(\theta)$ shifts to the right side, i.e., the number of contacts on the mobilized plane increases in the positive

zone of θ where the angle θ is effective to resist shearing(Matsuoka, 1974). Essentially, the shift of $N(\theta)$ distribution on the mobilized plane to the positive zone of θ is the same as the concentration of contact normals in the major principal stress direction in **Fig.14.**

Now, we consider the reason why the contact normals concentrate around the major principal stress direction and $N(\theta)$ is one-sided to the positive zone of θ. **Figure 16(a)** shows the frequency distribution of contact normals which have newly been generated during shear, $M_g(\alpha)$, while **Figure 16(b)** shows the frequency distribution of contact normals which have disappeared during shear, $M_d(\alpha)$. The contact corresponding to $M_g(\alpha)$ and $M_d(\alpha)$ is called an "generated contact" and "disappearing contact", respectively (Matsuoka and Takeda,1980). It is interesting to find that the "generated contact" normals concentrate in the major principal stress direction, while the "disappearing contact" normals concentrate in the minor principal stress direction. This is considered to be the reason of the concentration of contact normals in the major principal stress direction as shown in **Figure 14.** Furthermore, **Figures 17(a)** and **(b)** show the "generated contact" $N_g(\theta)$ and the "disappearing contact" $N_d(\theta)$ on the mobilized plane, respectively. Similarly, it is interesting to notice that $N_g(\theta)$ concentrates in the positive zone of θ, while $N_d(\theta)$ concentrates in the negative zone of θ. This is the reason why the distribution of $N(\theta)$ on the mobilized plane shifts to the positive zone of θ, i.e., the effective direction to resist shearing.

Distribution of Change in Contact Normal Direction on Mobilized Plane

Yamamoto et al.(1994,1995) performed a biaxial test on assemblies of aluminum rods using DEM, and found from the micromechanical observation that the change in contact normal directions ξ ,which arises along the mobilized plane, is proportional to the shear-normal stress ratio $\tau(\theta)/\sigma_N(\theta)$ on the contact plane expressed by the following form:

$$\frac{\tau(\theta)}{\sigma_N(\theta)}=\frac{\sin\phi_{mo}\cos(2\theta-\phi_{mo})}{1+\sin\phi_{mo}\sin(2\theta-\phi_{mo})} \quad (6)$$

Herein, we study the distribution of the change in contact normal directions ξ on the mobilized plane in the case of the simple shear test, as shown in **Fig.18**. It is indicated from **Fig.18** that the distribution of the change in contact normal directions ξ on the mobilized plane is also nearly proportional to the shear-normal stress ratio $\tau(\theta)/\sigma_N(\theta)$ expressed by Eq.(6) in the case of the simple shear test.

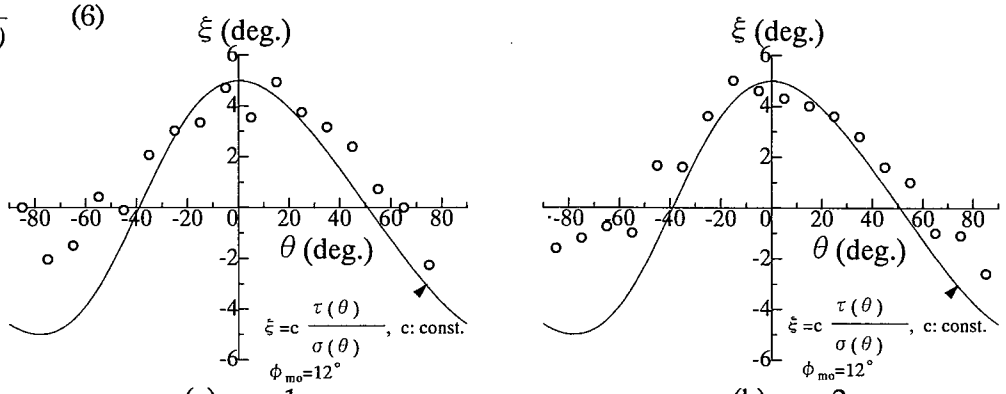

Fig.18 Distribution of change in contact normal directions on the mobilized plane

CONCLUDING REMARKS

The conclusions from this study may be summarized as follows:

(1) From a microscopic view, the macroscopic shear-normal stress ratio τ/σ_N on the mobilized plane is related to not only the distribution of the interparticle contact angle, but also the distribution of the interparticle contact force, which is expressed by $\bar{x}$ (Eq.2) in this paper. There exists a difference δ between $\bar{x}$ and the average interparticle contact angle $\bar{\theta}$ on the mobilized plane. This difference δ is about 7° in our simulation results of the simple shear test on aluminum rod mass and almost changeless during shear , independent of the height and the initial void ratio of the specimen. The stress-dilatancy relationship of the granular material on the mobilized plane is reviewed by Eq.(5) through $\bar{\theta}$ and δ, in which $\tan\delta$ corresponds to the value of τ/σ_N when $d\varepsilon_N/d\gamma=0$.

(2) With the increase in shear force during the simple shear test, the contact normals tend to concentrate toward the major principal stress direction. The reason for this is that the "generated

contact" normals concentrate around the major principal stress direction and the "disappearing contact" normals concentrate around the minor principal stress direction, as shown in **Fig.16**.

(3) In the simple shear test, it is also confirmed that the distribution of the change in interparticle contact angle is proportional to the distribution of macroscopic shear-normal stress ratio on the contact plane, which was found by Yamamoto et al.(1994,1995) in the biaxial compression test using DEM.

ACKNOWLEDGEMENTS

The authors wish to express their sincere gratitude to Dr. S. Yamamoto of Obayashi Corporation for his great help in DEM calculation.

REFERENCES

1) Christoffersen, J., Mehrabadi, M.M. and Nemat-Nasser, S.(1981): "A micromechanical description of granular material behavior," J. Appl. Mech., Vol.48,No.2, pp.339-344.
2) Matsuoka, H.(1974): "A microscopic study on shear mechanism of granular materials," Soils and Foundations, Vol.14, No.1, pp.29-43.
3) Matsuoka, H. and Takeda, K.(1980): "A stress-strain relationships for granular materials derived from microscopic shear mechanism," Soils and Foundations, Vol.20, No.3, pp.45-58.
4) Matsuoka, H. and Yamamoto, S.(1994): " A microscopic study on shear mechanism of granular materials by DEM," Journal of Geotechnical Engineering, JSCE, No.487/Ⅲ-26,pp.167-175(in Japanese).
5) Matsuoka, H., Liu, S.H., Ueno, Y. and Kodama, H.(1998): "Microscopic study on stress-dilatancy relation of granular materials in simple shear by DEM," Proc. Of 33th Japan National Conf. On Geotechnical Engineering (in Japanese, to be presented).
6) Matsuoka, H., Liu, S.H., Ueno, Y. and Kodama, H.(1998): "A microscopic study on shear mechanism of granular materials in simple shear test based on DEM simulation,", Proc. Of the 53th Annual Conf. Of the Japan Society of Civil Engineers (in Japanese, to be presented).
7) Oda,M. and Konishi, J.(1974): "Microscopic deformation mechanism of granular material in simple shear," Soils and Foundations, Vol.14, No.4, pp.25-38.
8) Oda,M. and Konishi, J.(1974): "Rotation of principal stresses in granular material during simple shear," Soils and Foundations, Vol.14, No.4, pp.39-53.
9) Yamamoto, S. and Matsuoka, H.(1994): " A relationship between fabric changes and shear strain of granular materials under shear," Journal of Geotechnical Engineering, JSCE, No.505/Ⅲ-29,pp.219-228(in Japanese).
10) Yamamoto, S.(1995): "Fundamental study on mechanical behavior of granular materials by DEM," Dr. Eng. Thesis, Nagoya Institute of Technology(in Japanese).